OPTIMIZATION OF GRI-MECH 3.0 MECHANISM USING HCCI COMBUSTION MODELS AND GENETIC ALGORITHM

A. Yousefzadi Nobakht, R. Khoshbakhi Saray and G. Soleimani Astiar*

Department of Mechanical Engineering, Sahand University of Technology
P.O. Box 51335-1996, Tabriz, Iran
a.y.nobakht@gmail.com - khoshbakhti@sut.ac.ir - soleimani.ghasem@yahoo.com

*Corresponding Author

(Received: August 22, 2009 – Accepted in Revised Form: April 23, 2011)

Abstract This paper presents a modeling study of a CNG Homogenous Charge Compression Ignition (HCCI) engine using a single-zone and a multi-zone combustion model. Authors' developed code is able to predict engine combustion and performance parameters in closed part of the engine cycle. As detailed chemical kinetics is necessary to investigate combustion process in HCCI engines, therefore, GRI-mech3.0 mechanism was used which includes 53 chemical species and 325 reactions for natural gas combustion. Although, single-zone model is useful to parametric study on variation of some engine combustion parameters such as start of combustion (SOC); But, it could neither be able to accurately predict other engine combustion related parameters nor engine performance and emission parameters. Hence, a multi- zone combustion model was developed to predict those parameters accurately. GRI-mech 3.0 combustion mechanism was developed for natural gas combustion without considering Exhaust Gas Recirculation (EGR). To consider the effect of EGR on HCCI combustion, the mechanism's rate coefficients should be optimized. These coefficients were optimized using a developed genetic algorithm code. Predicted values show good agreement with corresponding experimental values for whole ranges of engine operating conditions.

Keywords HCCI Combustion, Chemical Kinetics, Single-Zone Model, Multi-Zone Model, Genetic Algorithm

چکیده کار حاضر به‌منظور مطالعه روی موتورهای HCCI کمک یک مدل احتراقی تک منطقه‌ای و یک مدل چند منطقه‌ای، انجام شده است. کد توسعه یافته قادر به پیش بینی پارامترهای احتراقی و عملکردی موتور در سیکل بسته موتور می باشد. از آنجایی که سینتیک شیمیایی مفصل در بررسی احتراق HCCI امری ضروری است، برای این منظور مکانیزم شیمیایی GRI-mech 3.0 شامل 53 گونه شیمیایی و 325 واکنش شیمیایی در نظر گرفته شده است. گرچه مدل‌های تک منطقه‌ای ابزار مناسبی برای بررسی پارامتریک روی تغییرات یک سری پارامترهای احتراقی از قبیل لحظه ی شروع احتراق می‌باشد ولی این مدل‌ها قادر به پیش بینی دقیق مقادیر دیگر پارامترهای احتراقی و عملکردی موتور نیستند. بنابراین یک مدل چند منطقه‌ای برای پیش بینی این پارامترها توسعه یافته است. مکانیزم شیمیایی GRI-mech 3.0 برای گاز طبیعی و بدون در نظر گرفتن EGR توسعه یافته است. برای مد نظر قرار دادن تاثیر EGR در احتراق HCCI پارامترهای مربوط به نرخ انجام واکنش‌های شیمیایی در مکانیزم GRI-mech 3.0 بایستی بهینه می‌شدند. این پارامترها به کمک یک الگوریتم ژنتیک بهینه‌سازی شدند. نتایج پیش بینی شده در تمام شرایط عملکردی در نظر گرفته شده تطابق خوبی با نتایج آزمایشگاهی دارند.

1. INTRODUCTION

Operating an engine using the Homogeneous Charge Compression Ignition (HCCI) technology can significantly reduce NO_x and particulate matter emissions while keeping thermal efficiency high [1,2]. However, HCCI generates more unburned hydrocarbons (UHC) than traditional engines and operates with lower Indicated Mean Effective Pressure (IMEP) [3,4]. Inability to control the initiation and rate of combustion over the required speed and load range of engines [5] and low IMEP are limiting the commercialization of the HCCI engines.

In recent years, HCCI engines received many researchers' attention and many papers have been published in these years. A major portion of these publications are related to modeling studies on HCCI engines. Most of modeling challenges can be divided into three major groups:

1. single-zone models
2. multi-zone models
3. CFD models

As, it is generally accepted that HCCI combustion characteristics are controlled by chemical kinetics, considering detailed chemical kinetics in HCCI engine modeling can improve the model results. In CFD models, coupling CFD codes with detailed chemical kinetics leads to a long run time. Therefore, single-zone and multi-zone models are more common than CFD models. Additionally, the use of fluid mechanics codes is most important in operating conditions in which the charge is not homogeneous and fuel mixing and evaporation may have a significant effect on the combustion process [6]. Some of recent studies are summarized as follows:

Aceves, et al [6] developed a multi-zone model coupled with CFD code using KIVA and HCT. The authors studied the effect of equivalence ratio and inlet temperature on SOC in HCCI engines.

Fiveland, et al [7] introduced a detailed chemical kinetics single-zone combustion model. The authors used CHEMKIN library for chemical kinetics modeling. They modeled HCCI engine for natural gas and hydrogen fuels. They performed a parametric study on HCCI engine.

Easley, et al [8] described engine's combustion, performance and emission parameters for iso-octane, methane and n-heptane fueled engines using a MZCM and detailed chemical kinetics. To predict NOx emissions accurately some reactions have been added to reaction mechanisms.

Ogink, et al [9] modeled the complete cycle of a HCCI engine using SENKIN and AVL BOOST software packages. The initial conditions at IVC calculated by AVL BOOST and fed to a MZCM which used SENKIN. Again, AVL BOOST was employed at the end of expansion stroke to model gas exchange process. Because of emission calculation at EVO, engine emissions were over predicted.

Babajimopoulos, et al [10] used Variable Valve Timing (VVT) method of controlling HCCI combustion timing as a theoretical study. Authors coupled a MZCM and a CFD model in their study. CFD part was modeled using KIVA-3V and detailed chemical kinetics was modeled using CHEMKIN package. KIVA-3V was used for calculating gas exchange and expansion steps. Compression and combustion steps were modeled using CHEMKIN. The authors considered both temperature and equivalence ration stratification inside the cylinder to predict engine emissions in a better way. They found that each zone's ignition is a function of its temperature and the zone which has the highest temperature ignites earlier.

Kongsereeparp, et al [11] introduced a new method of setting initial conditions at IVC for multi-zone HCCI combustion modeling. The authors assumed an "S" shaped in-homogeneity in the engine cylinder. This assumption was raised from the schematic of flow behavior during the intake stroke and developed model based on this assumption has good agreement with experimental results.

Komninos, et al [12] developed a new MZCM in which heat and mass transfer was taken into account simultaneously but they didn't use detailed chemical kinetics for HCCI combustion modeling. They study the effect of compression ratio and temperature at IVC on SOC and peak pressure. Increasing the temperature at IVC leads to earlier SOC and higher peak pressure, increasing compression ratio has the same effect on these two parameters. Later the authors published a parametric study on a hydrogen HCCI engine using the aforesaid model [13].

The present contribution describes a single-zone and a five-zone combustion models were developed to investigate HCCI combustion in natural gas fueled engines. In multi-zone model both heat and mass transfer are considered. At first for a specific operating condition, GRI-mech3.0 mechanism's rate coefficients were optimized using genetic algorithm. Then, Single-zone and multi-zone model results were compared with experimental data for that case and two other cases for validation of the model. Experimental data was recorded from a Co-operative fuel research (CFR) single-cylinder engine.

2. DESCRIPTION OF THE COMBUSTION MODELS

In single-zone model, it is assumed that the mixture in the cylinder is homogeneous during the cycle. Pressure and temperature assumed to be uniform in the cylinder. When combustion starts,

whole mixture burns at the same time and all of fuel energy release in a short period of time. Single-zone model cannot describe unburned or partially burned regions of the combustion chamber. Therefore, these models usually over predict maximum pressure and temperature and subsequently NOx emission and also under predict CO and UHC emissions.

In order to improve single-zone model limitations, a five-zone model was developed. As shown in Figure 1, five-zone model includes two core zones, one zone for cylinder wall, one zone for cylinder head and one zone for piston crown.

Core volume (V_{core}) is perfectly centered within the charge, forming an inner cylinder of gas that is surrounded by an outer concentric shell of gas with thickness t1.

To model a physical boundary layer, it is assumed that each zone becomes successively thinner as it approaches an in-cylinder surface. This procedure for allocating zones is also consistent with the natural temperature profiles that develop within the charge during the compression stroke and leading up to combustion. Another parameter, which is essential to calculate the remaining zone thicknesses, is the geometric ratio defined by R. The value of R indicates each successive zone is how much thinner than previous zone's thickness. V_{core}, a fraction of total cylinder volume, and R are adjustable model parameters.

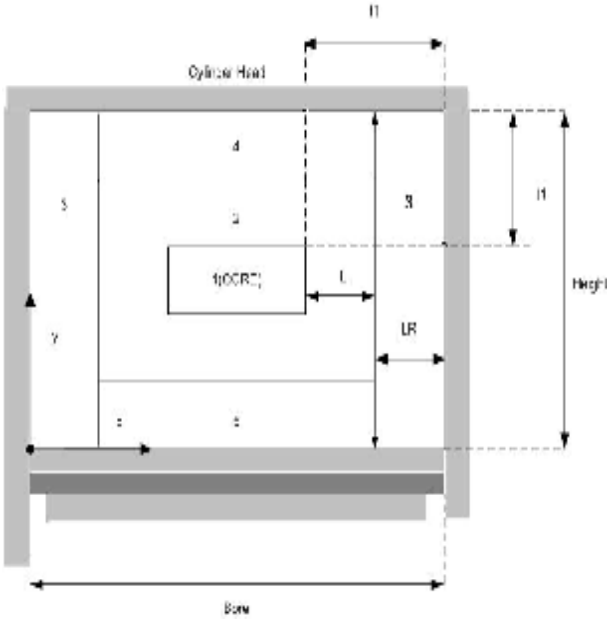

Figure 1. Zone configuration.

3. GOVERNING EQUATIONS

Due to the mass conservation and modeling of the closed part of combustion, from inlet valve closing (IVC) to exhaust valve opening (EVO), in-cylinder mass remains constant. Therefore:

$$\frac{dm_{tot}}{dt} = 0 \tag{1}$$

Mass is transferred between zones to maintain the pressure uniform inside the combustion chamber as follows:

$$\frac{dm_k}{dt} \neq 0 \qquad K = 1,...,N_Z \tag{2}$$

$$\sum_{K=1}^{N_Z} m_k = m_{tot} \qquad K = 1,...,N_Z \tag{3}$$

The cylinder pressure is calculated at each crank angle (CA) step using the ideal gas relation for all the zones:

$$PV_k = \frac{m_k}{MW_k} R_u T_k \qquad K = 1,...,N_Z \tag{4}$$

Cylinder volume changes relative to time as follows:

$$\frac{dV}{dt} = V_c[\frac{1}{2}\left(r_c - 1\right)\left(\sin q \frac{dq}{dt} - \frac{1}{2}\left(R_C{}^2 - \sin^2 q\right)^{-\frac{1}{2}}(-\sin 2q)\frac{dq}{dt}\right)] \tag{5}$$

Energy conservation equation and net rate of production equation for each species are also as follows:

$$m_k \overline{c_u^k} \frac{dT_k}{dt} = -m_k \sum_{i=1}^{N_s} U_i \frac{dY_{i,k}}{dt} - P\frac{dV_k}{dt} + \frac{dQ_k}{dt} \tag{6}$$

$$\frac{dY_{i,k}}{dt} = \frac{\dot{w}_{i,k} MW_i}{r_k} \tag{7}$$

All properties in each zone of a MZCM were considered to be uniform at IVC and calculated based on ideal gas theory.

Convection from in-cylinder mixture to cylinder wall in both multi-zone and single-zone models was described using Woschni correlation [14].

$$h_c(t) = bHeight(t)^{-0.2} P(t)^{0.8} T(t)^{-0.73} v(t)^{0.8} \quad (8)$$

The Woschni correlation was developed from a regression of direct injection diesel engine data and is essentially a linearized radiative/convective relation that will greatly over-predict heat transfer in a lean burn, premixed, nonsooting engine [8]. Consequently, to predict heat loss in a better way, coefficients of the Woschni correlation were modified in this model.

Heat is transferred between zones with a mechanism similar to conduction. Therefore, the heat flux is based on the temperature difference of the neighboring zones and on their mean distance as follows:

$$\dot{q} = -K_{tot} \frac{dT}{dy} \quad (9)$$

The total conductivity in Equation 2 is calculated based on the approach of Komninos [15] and is the sum of a laminar and a turbulent component.

$$k_{tot} = k_l + k_t \quad (10)$$

The ratio of turbulent to laminar conductivity is calculated using the following formula:

$$\frac{k_t}{k_l} = \frac{\mathrm{Pr}_l}{\mathrm{Pr}_t} \frac{m_t}{m_l} \quad (11)$$

Equation 4 presupposes swirl dominated flows and is used in the absence of other data. The viscosity ratio of Equation 4 is calculated from the following relation:

$$\frac{m_t}{m_l} = ky_n^+ \left[1 - \exp(-2aky_n^+)\right] \quad (12)$$

and

$$y_n^+ = \frac{u^*}{m_w} \int_0^u r\, dy_n \quad (13)$$

Where k=0.41 is the Von Karman Constant, α=0.06 and y_n^+ is the normal distance from the wall. The characteristic velocity is considered to be proportional to engine speed.

4. EXPERIMENTAL SET-UP AND ENGINE SPECIFICATIONS

The experiments were conducted using a Waukesha Co-operative fuel research (CFR) single-cylinder engine. CFR engine is a standard engine with Bore × Stroke (mm) of 82.6 × 114.3 and displacement of 612 cc. Throttle was kept wide open. A heater was installed inside the intake manifold in order to control the intake mixture temperature when needed. Intake mixture consisted of air, natural gas and exhaust gas recirculation (EGR). Intake mixture temperature was set at constant value and was monitored just before intake valve. EGR line was taken immediately after exhaust port and returned to intake manifold after the heater and before the fuel injectors. EGR was controlled by a manual butterfly valve. A Kistler 6043A water cooled pressure transducer was used to acquire pressure signal on a 0.1 CAD resolution. Table 1 summarizes the engine specifications for the current experiments.

5. DESCRIPTION OF THE COMPUTATIONAL PROCEDURE OF MULTI-ZONE MODEL

Models was developed using FORTRAN programming language. The solver code solves the unknown variables (mass fraction for each chemical species and temperature for each zone) sequentially (zone by zone) from zone 1 to zone 5, for a user-defined time step. Time step was fixed at 0.1 CA for compression and expansion processes and 0.05 for auto ignition process (40^o CA before top dead center to 40^o after top dead center).

The computational procedure of the multi-zone code is shown in Figure 2. It can be seen that the calculation for each CA step is completed in two stages. First, mass of the zones was assumed constant (i.e. the mass transfer among zones was

TABLE 1. CFR Engine Specifications.

Engine Model	Waukesha CFR
Engine Type	Water cooled, Single cylinder
Combustion Chamber	Disk Cylinder Head, flat-top piston
Displacement (cc)	612
Throttle	Fully Open
Main Fuel	CNG
Compression Ratio	13.8
Bore (cm)	8.26
Stroke (cm)	11.4
Displacement (cc)	611
Connecting Rod Length (cm)	24
IVO (CA)	10
IVC (CA)	214
EVO (CA)	500
EVC (CA)	735

not considered). In order to estimate temperature and composition of the zones, the first law of thermodynamics, simultaneously, with the net rate of production equation for each species was applied.

In the second stage, initially, the cylinder total pressure was calculated. Then, by considering ideal gas law and each zone's defined volume, each zone's new temperature and mass were calculated.

If the computed mass in the second stage differs considerably with considered tolerance of the first stage, in order to equalize pressure, mass transfer among the zones takes place. Because of mass transfer, energy transfer among the zones occurs. Thus, the first law of thermodynamics and the mass conservation step should be calculated again. Single-zone model procedure is like multi-zone model. But in single zone-model the number of zones is one, therefore there is no mass transfer phenomenon.

6. GENETIC ALGORITHM

In the current study, genetic algorithm (GA) was applied using a FORTRAN90 code. GA code first, recalls GA input parameters from a file, and then it produces a population randomly, within the range +/-15% around the original values, and by recalling MZCM, it performs an initial estimate of fitness function using this population. After calculating fitness function, GA changes the chemical mechanism parameters and repeats this procedure again and again until it attains maximum generation size.

Applied GA calculates fitness function using a weighting method in which weights (w_i) were selected based on functions importance. Fitness function was considered as follows:

$$\text{Fitness Function} = \sum_{i=1}^{2}\left[w_i \times \left| \frac{X_{i,code} - X_{i,test}}{X_{i,test}} \right| \right] \qquad (14)$$

The term $\left| \frac{X_{i,code} - X_{i,test}}{X_{i,test}} \right|$, is the i^{th} target function in which, $X_{i,code}$ is the estimated i^{th} variable via MZCM and $X_{i,test}$ is the experimental attained quantity for i^{th} variable. In this work the concerned functions were related to maximum pressure and indicated work of each working cycle. The optimized rate coefficients are available in appendix A. Other parameters which have been used in genetic algorithm code are shown in Table 2.

7. RESULTS AND DISCUSSION

This section verifies multi-zone and single-zone models results. As mentioned above GRI-mech 3.0 chemical mechanism's rate coefficients were optimized for one case (case 1 in Table 3.) and then the optimized mechanism were used to model two other engine operating conditions (cases 2 and 3 in Table 3.) to validate the developed model results.

Figure 3 shows a comparison between experimental and predicted pressure traces for the three cases being considered. For each experimental data, two predicted pressure traces are shown. The predicted pressure traces were calculated with

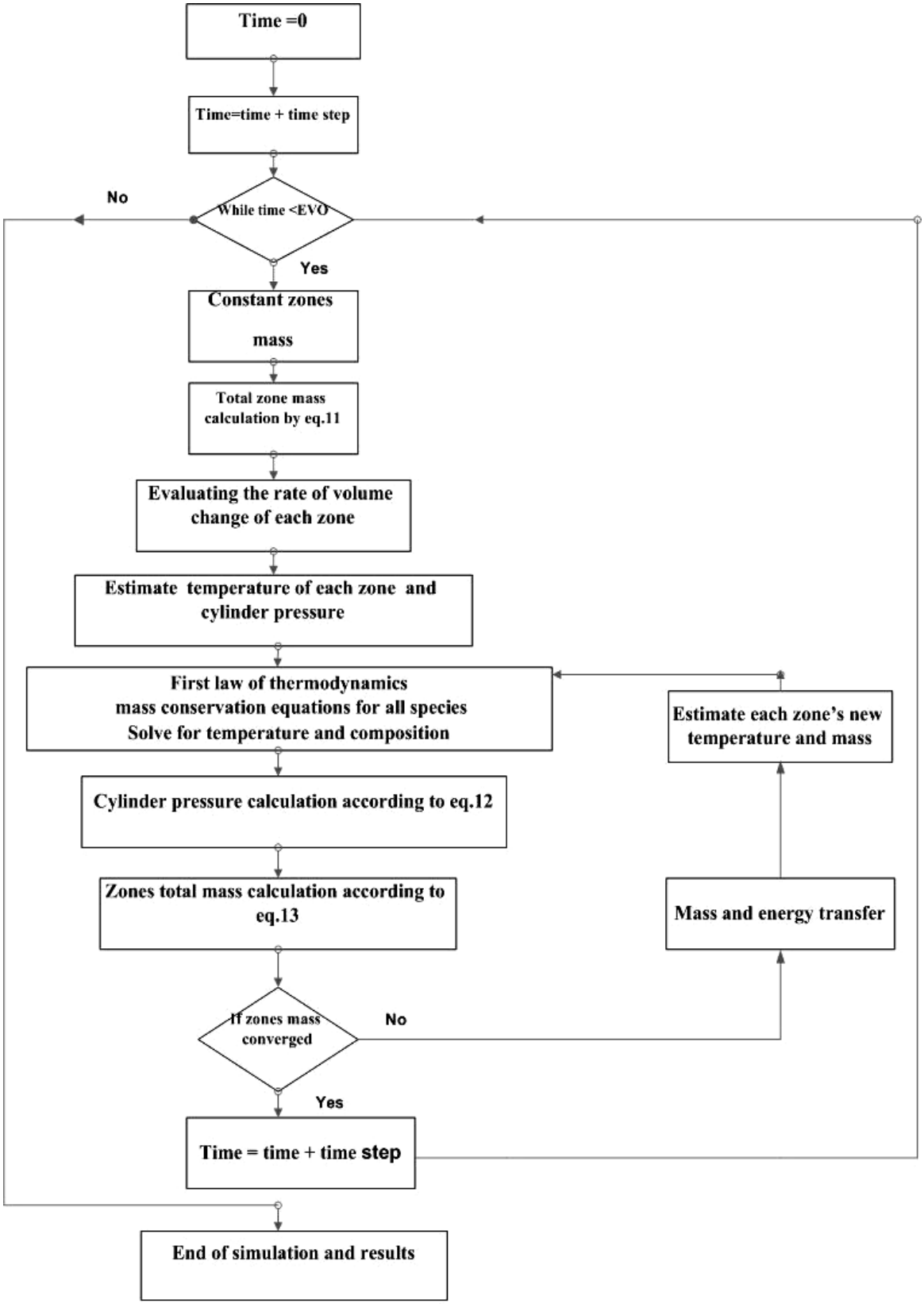

Figure 2. MZCM flow chart.

TABLE 2. Genetic Algorithm Parameters.

Crossover Probability (Pc)	0.5
Mutation Probability (Pm)	0.02
Population Number (n-population)	50
Maximum Produced Population	300

TABLE 3. Operating Conditions for Considered three Cases.

Case	1	2	3
Equivalence Ratio Φ	0.55	0.48	0.29
Air mass rate (g/s)	2.94	3.30	3.35
RPM	800	800	800
T_{IVC} (K)	413	413	413
P_{IVC} (bar)	1.56	1.58	1.57
% EGR	30.52	21.15	9.68
Compression Ratio	17.25	17.25	17.25

single-zone and multi-zone combustion models. As discussed previously, single-zone model assumes a homogenous mixture inside the cylinder and therefore, predicts a very short burning duration and a high peak pressure [16].

MZCM takes temperature and composition distributions into consideration and has better results in comparison with SZCM. According to Figure 3, MZCM can reasonably capture pressure history.

Figure 4 Shows Heat Release Rate (HRR) graphs for three considered operating conditions. According to graphs, it can be realized that in SZCM combustion starts earlier than MZCM, because boundary layer was not included in SZCM and this model predicts less heat loss than MZCM.

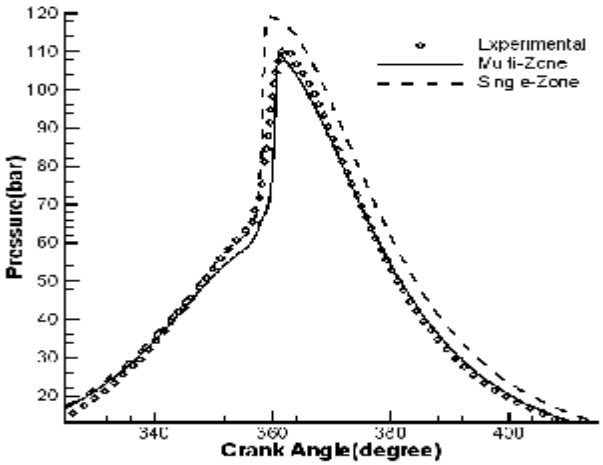

Case 1

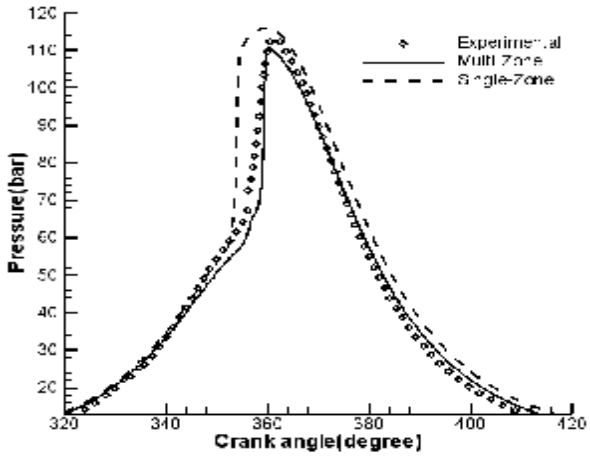

Case 2

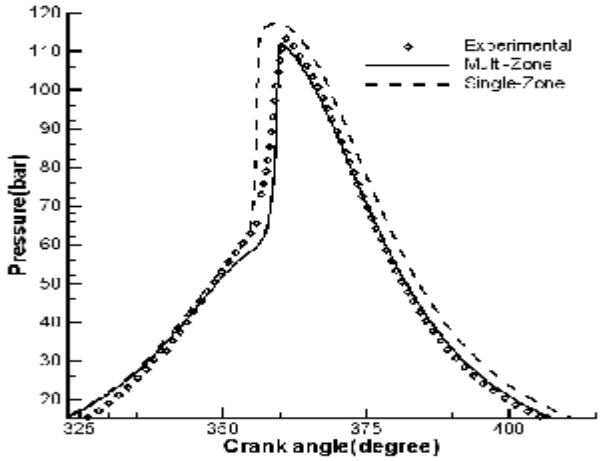

Case 3

Figure 3. Pressure history of three different operating conditions.

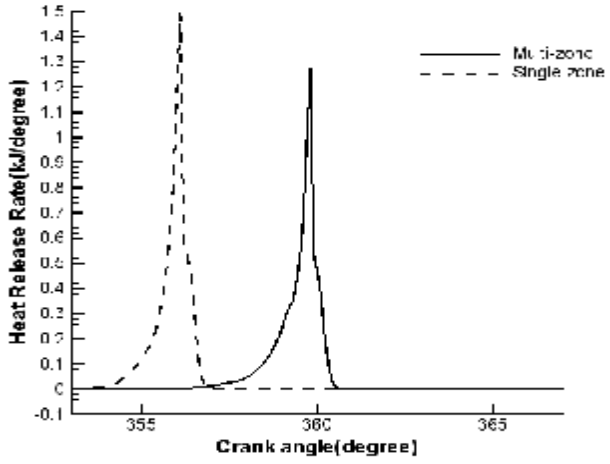

Case 1

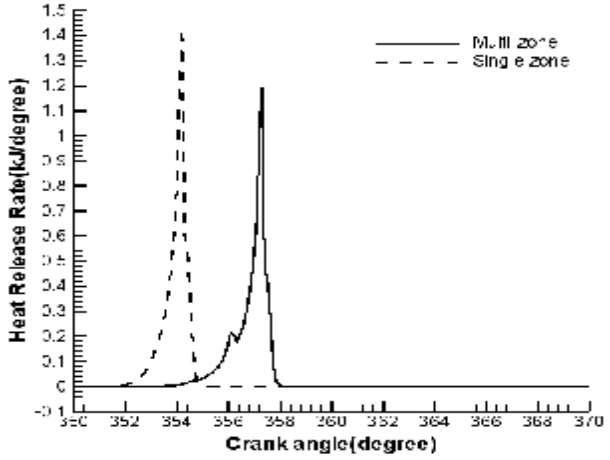

Case 2

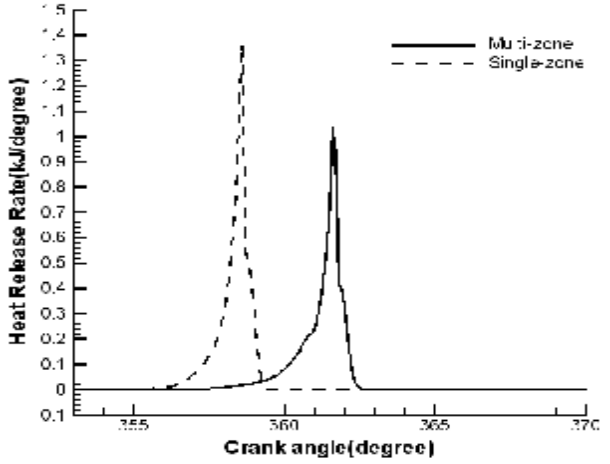

Case 3

Figure 4. Heat Release Rate of three different operating conditions.

Then mixture warms up faster during compression stroke and ignites earlier. Due to lumped properties assumption in SZCM, there is no unburned hydrocarbon (UHC) and all of the fuel burns in a short period of time. It causes a thinner and higher heat release rate diagram for SZCM.

8. CONCLUSION

In this work a modeling study has been carried out to compare single-zone and multi-zone models abilities. Because of importance of chemical kinetic in HCCI combustion, detailed chemical kinetics was considered in both models. Improvement of the existence chemical kinetic mechanism is necessary due to addition of EGR in the cylinder charge. For this purpose, the rate coefficients of GRI-mech 3.0 mechanism were optimized using GA.

The following conclusions have been drawn:

1. The GA might be used in the hydrocarbons chemical kinetic mechanism development by the reactions rate coefficients adjustment.
2. Fitness function, on the basis of maximum pressure and indicated work, might be employed, as an effective parameter, in the proposed mechanism improvement in order to forecast combustion and performance parameters by the use of both combustion models.
3. According to comparison of modeling results with experimental data, MZCM have better performance than SZCM.
4. Due to lumped properties assumption in SZCM, there is no unburned hydrocarbon (UHC) and all of the fuel burns in a short period of time. It causes a thinner and higher heat release rate diagram for SZCM.

9. NOMENCLATURE

Height	Cylinder height (m)
h_c	Convection heat transfer coefficient ($W/m^2 k$)
K	Thermal conductivity (W/m k)
k	Karman constant

L	Thickness (m)
m	Mass (Kg)
m_k	The amount of mass inside the kth zone (Kg)
MW_k	Average zone Molecular weight of the kth zone (Kg/Kmole)
N_S	Total number of species
N_Z	Total number of zones
P	In-cylinder Pressure (Pa)
Q_k	Heat transfer into/out of the kth zone (J)
R	Geometric ratio
R_C	Ratio of connecting rod length to crank radius
r_c	Compression ratio
Z	Number of zones
R_u	Universal Gas Constant (8.314 J/mole K)
t	Time measured reference to TDC (t @ TDC = 0 sec)
t_1	Thickness (m)
T	Temperature (K)
T_k	Mixture temperature of the kth zone (K)
U_i	Internal energy of the i^{th} species (J)
V	In-cylinder volume (m^3)
V_c	Clearance volume (m^3)
V_k	Volume inside the k^{th} zone (m^3)
w_i	Weighting factor of the ith target function
y	Distance (m)
$Y_{i,k}$	Mass fraction of the ith species in the k^{th} zone

Greek

b	Correcting factor for heat transfer to the wall
n	Velocity (m/sec)
$\dot{w}$	Molar rate of production (moles/(cm^3 sec))
f	Equivalent ratio
r	Density (Kg/m^3)
$\overline{c_n^{\,k}}$	Specific heat constant (at constant volume) of intake mixtures inside the k^{th} zone (J/Kg K)
q	Crank angle (Degree)

Subscripts

l	Laminar
n	Normal
t	Turbulent
tot	Total
w	Wall

Superscripts

+	Dimensionless value
*	Characteristic value

Abbreviations

ATDC	After top dead center
BTDC	Before top dead center
CA	Crank angle
CFR	Co-operative fuel research
CNG	Compressed natural gas
EGR	Exhaust gas recirculation
EVO	Exhaust valve opening
GA	Genetic Algorithm
HCT	Hydrodynamics, Chemistry and Transport
HRR	Heat release rate
IVC	Inlet valve closing
MZCM	Multi-zone combustion model
RPM	Revolutions per minute
SZCM	Single-zone combustion model
SOC	Start of combustion
UHC	Unburned Hydro Carbon

10. APPENDIX A

Optimized GRI-mech 3 Mechanism Rate coefficients are expressed in the form:

$$K = A \times T^{b} \times \exp(-\frac{E}{RT})$$

For concentration units mol/cm 3 and time in s. E is given in cal/mol.

*reaction numbers are similar to GRI-mech 3.0 chemical mechanism also enhanced factors and TROE parameters are same as the original mechanism.

No.	A	b	E	No.	A	b	E
1	1.36E+17	-1.07116	0.00E+00	164	249007.7	2.219272	5056.426
2	4.90E+17	-0.85056	0.00E+00	165	5365181	1.929471	4977.451
3	38903.12	2.426748	3096.574	166	1.46E+18	-1.08351	7874.896
4	1.91E+13	0.00E+00	0.00E+00	167	1.83E+17	-0.86351	9141.279
5	10374077	2.13401	2094.316	168	1.28E+13	0.00E+00	225.8045
6	5.63E+13	0.00E+00	0.00E+00	169	1.74E+13	0.00E+00	494.038
7	7.67E+13	0.00E+00	0.00E+00	170	4.88E-13	7.041895	-1511.62
8	1.53E+13	0.00E+00	0.00E+00	171	1.09E+13	0.00E+00	-336.545
9	1.69E+13	0.00E+00	0.00E+00	172	5.81E+10	1.014565	990.2779
10	5.32E+13	0.00E+00	0.00E+00	173	5.02E+16	-1.29856	578.3126
11	8.92E+08	1.455789	4246.819	174	8.54E+12	0.472726	37404.41
12	1.77E+10	0.00E+00	1025.313	175	8.84E+11	0.00E+00	1848.151
13	3.04E+13	0.00E+00	0.00E+00	176	3.13E+12	0.00E+00	441.6588
14	3.32E+13	0.00E+00	0.00E+00	177	1.03E+13	0.00E+00	0.00E+00
15	4.24E+13	0.00E+00	1729.423	178	2.3E+13	0.00E+00	182.495
16	9.22E+12	0.00E+00	0.00E+00	179	8.43E+09	1.057668	3071.453
17	1.04E+13	0.00E+00	0.00E+00	180	3.8E+13	0.00E+00	202.7872
18	371338.4	2.452066	1575.878	181	1.44E+12	0.00E+00	5466.545
19	146772.1	2.581122	2752.03	182	2.58E+13	0.00E+00	10547.48
20	4.98E+13	0.00E+00	0.00E+00	183	4.27E+14	0.00E+00	8398.748
21	12636773	2.000655	924.5181	184	2.08E+12	0.00E+00	9579.932
22	4.39E+19	-1.46451	13163.26	185	6.95E+10	0.00E+00	26065.75
23	6444037	2.182004	958.4007	186	2.04E+12	0.00E+00	-225.049
24	3.02E+13	0.00E+00	0.00E+00	187	1.20E+20	-1.53783	0.00E+00
25	13675113	1.933774	116.8222	188	3.44E+12	0.00E+00	-113.951
26	2.44E+13	0.00E+00	0.00E+00	189	1.38E+14	0.00E+00	180.2627
27	77759099	1.927692	3020.181	190	3.81E+13	0.00E+00	0.00E+00
28	8.56E+13	0.00E+00	0.00E+00	191	3.35E+13	0.00E+00	147.2685
29	9.49E+12	0.00E+00	3497.714	192	2.19E+13	0.00E+00	0.00E+00
30	1.64E+12	0.00E+00	607.5207	193	2.06E+09	1.233495	0.00E+00
31	2.28E+12	0.00E+00	21685.4	194	510953.3	1.727546	3580.343
32	1.05E+14	0.00E+00	17110.21	195	1166285	1.341217	52.75
33	3.03E+18	-0.96097	0.00E+00	196	1.65E+13	0.00E+00	0.00E+00
34	2.10E+19	-1.33419	0.00E+00	197	2.06E+13	0.00E+00	7807.114
35	1.29E+19	-0.67576	0.00E+00	198	2.42E+13	-0.25419	0.00E+00
36	2.75E+19	-1.32632	0.00E+00	199	3.85E+14	-0.39128	0.00E+00
37	6.46E+17	-0.7333	0.00E+00	200	3.04E+12	0.00E+00	0.00E+00
38	2.40E+16	-0.76755	9796.011	201	3.82E+13	0.00E+00	0.00E+00
39	1.12E+18	-1.09988	0.00E+00	202	4.59E+13	0.00E+00	2030.487
40	9.76E+16	-0.56216	0.00E+00	203	76900949	1.349754	-257.463
41	5.87E+19	-1.40926	0.00E+00	204	3.49E+08	0.00E+00	0.00E+00
42	6.16E+20	-2.0372	0.00E+00	205	1.27E+14	-9.52E-02	2721.911
43	2.44E+22	-1.73321	0.00E+00	206	5.27E+12	0.00E+00	0.00E+00

44	4.3E+12	0.00E+00	310.436	207	2.13E+13	0.00E+00	0.00E+00
45	4.26E+13	0.00E+00	616.9713	208	6.83E+13	0.00E+00	0.00E+00
46	9.59E+13	0.00E+00	305.7378	209	5.55E+13	0.00E+00	0.00E+00
47	13244274	1.890831	2766.963	210	1.74E+13	0.00E+00	0.00E+00
48	1.06E+13	0.00E+00	1874.851	211	2.7E+13	0.00E+00	0.00E+00
49	1.74E+14	0.00E+00	0.00E+00	212	4.95E+19	-1.42499	333.9986
50	6.12E+14	0.00E+00	0.00E+00	213	2.25E+13	0.00E+00	0.00E+00
51	2.64E+13	0.00E+00	0.00E+00	214	9.5E+11	0.700187	291.1989
52	1.54E+16	-0.49584	293.3834	215	12996153	2.024156	-546.246
53	5.8E+08	1.462564	4903.838	216	1.09E+13	0.00E+00	5791.008
54	1.24E+12	0.538712	-112.084	217	7.33E+13	0.00E+00	0.00E+00
55	8.21E+13	0.00E+00	0.00E+00	218	4.4E+13	0.00E+00	0.00E+00
56	6.19E+11	0.491854	1909.802	219	7.74E+12	0.00E+00	3906.449
57	5.59E+11	0.40246	1155.808	220	5.95E+12	0.00E+00	-227.982
58	64965425	2.06244	1268.233	221	267722.8	2.339563	987.799
59	1.13E+12	0.56154	40.07457	222	2.47E+13	0.00E+00	0.00E+00
60	2.2E+13	0.00E+00	0.00E+00	223	5.37E+13	0.00E+00	0.00E+00
61	1.8E+11	0.734312	-123.087	224	2.65E+12	0.00E+00	0.00E+00
62	3.04E+13	-7.66E-02	292.6947	225	1.76E+13	0.00E+00	0.00E+00
63	2.55E+12	0.522333	27.23729	226	1.94E+12	0.00E+00	9325.974
64	35846253	1.741417	833.1409	227	3.51E+14	0.00E+00	24256.95
65	1.8E+13	0.00E+00	0.00E+00	228	1.62E+17	-1.34197	327.6105
66	1.4E+12	0.429721	-48.2106	229	4.00E+18	-2.06976	461.5514
67	2.96E+14	-0.20807	527.8823	230	1.10E+29	-2.81984	54286.65
68	19316858	2.164906	2759.105	231	18132.97	2.698339	2416.712
69	4373210	2.181871	2393.222	232	5245.735	2.913411	2511.158
70	8.66E+16	-1.06365	0.00E+00	233	4.39E+09	1.695552	13582.34
71	4.8E+12	0.00E+00	1279.629	234	1247394	1.922734	7176.889
72	6.69E+12	0.235417	146.4412	235	4349.362	1.994232	2799.958
73	2.71E+13	0.00E+00	0.00E+00	236	182.1171	2.847804	5144.409
74	5.12E+11	0.514254	853.6694	237	2.81E+13	0.00E+00	0.00E+00
75	1346444	2.713206	6851.89	238	6.05E+13	0.00E+00	204.7839
76	4.65E+17	-0.90805	869.2745	239	6.06E+13	0.00E+00	21402.05
77	1.74E+12	0.00E+00	0.00E+00	240	2.78E+09	0.911938	11169.87
78	1.19E+08	1.690428	3663.135	241	3.36E+12	0.155183	0.00E+00
79	1.07E+14	0.00E+00	0.00E+00	242	1.11E+13	0.00E+00	39971.36
80	4.54E+13	0.00E+00	3961.202	243	1.05E+11	0.00E+00	29296.8
81	1.29E+13	0.00E+00	1641.431	244	1.78E+13	0.00E+00	0.00E+00
82	8.91E+12	0.00E+00	0.00E+00	245	3.26E+13	0.00E+00	0.00E+00
83	49235138	1.361545	43517.24	246	4.33E+13	0.00E+00	0.00E+00
84	2.27E+08	1.595758	1808.045	247	1.66E+13	0.00E+00	0.00E+00
85	7.71E+13	-0.35031	0.00E+00	248	2.47E+13	0.00E+00	0.00E+00
86	34221.68	2.064566	-990.439	249	3.29E+17	-1.43872	650.738
87	1.27E+13	0.00E+00	-283.483	250	3.09E+14	-0.78508	346.159

88	1.85E+12	0.00E+00	238.4616	251	4.12E+13	-0.35478	260.7156
89	1.67E+18	0.00E+00	15894.98	252	3.34E+17	-1.29762	707.1338
90	4.8E+13	0.00E+00	0.00E+00	253	3.08E+14	-0.71456	411.453
91	3.22E+13	0.00E+00	0.00E+00	254	4.35E+13	-0.31174	266.5523
92	1.71E+13	0.00E+00	0.00E+00	255	9.41E+13	0.00E+00	16119.78
93	12967298	2.023672	1689.981	256	9.63E+11	0.00E+00	9610.543
94	2.71E+13	0.00E+00	0.00E+00	257	2.08E+13	0.00E+00	0.00E+00
95	2.53E+18	-1.43034	672.7243	258	2E+12	0.00E+00	0.00E+00
96	47640317	1.652656	2491.938	259	1.14E+13	0.00E+00	0.00E+00
97	6.24E+17	-1.51891	726.5591	260	1.23E+13	0.00E+00	0.00E+00
98	92754615	1.595836	1744.172	261	8.5E+13	0.00E+00	0.00E+00
99	40942353	1.052312	38.09688	262	85690984	1.323059	4207.399
100	5.22E+13	0.00E+00	0.00E+00	263	1.35E+08	1.639688	20924.41
101	3.45E+09	1.341107	-191.438	264	2257290	2.253785	5998.516
102	4.53E+12	0.00E+00	0.00E+00	265	19166111	1.813897	1968.884
103	5.03E+12	0.00E+00	0.00E+00	266	104161.5	2.170442	6482.568
104	1318250	2.206741	-382.205	267	30468015	1.465031	1988.173
105	6779236	1.704746	759.0169	268	2918721	1.29057	2042.455
106	1.91E+13	0.00E+00	0.00E+00	269	1.07E+16	0.00E+00	39096.69
107	2.50E-04	4.81084	-576.362	270	2.27E+15	-0.63447	1320.062
108	532241.3	2.548153	6482.619	271	2.56E+11	0.153619	931.3979
109	31434017	2.075254	7444.366	272	1.76E+14	-0.69497	1530.484
110	4.58E-04	4.579373	-878.572	273	21747659	2.003791	991.4801
111	5.71E+12	0.00E+00	0.00E+00	274	1.01E+13	0.00E+00	0.00E+00
112	3748419	1.905099	1286.137	275	6.22E+14	-0.33997	124.1796
113	3789597	2.308933	454.9731	276	3.38E+12	0.127832	-46.9239
114	7.72E+12	0.00E+00	861.4193	277	604198.6	2.184272	5000.06
115	1.24E+11	0.00E+00	-853.593	278	49325284	1.362116	439.9209
116	4.37E+14	0.00E+00	6827.781	279	10439996	1.817474	3539.112
117	1.81E+13	0.00E+00	0.00E+00	280	1.07E+13	0.00E+00	7866.6
118	1E+12	0.00E+00	0.00E+00	281	6.05E+15	-0.64902	176.5455
119	3.6E+13	0.00E+00	0.00E+00	282	3.01E+12	0.00E+00	-396.264
120	1.57E+14	0.00E+00	11146.77	283	3.3E+12	0.00E+00	5322.268
121	6124409	1.961438	5165.675	284	3.58E+13	0.00E+00	0.00E+00
122	6.43E+13	0.00E+00	282.8085	285	6717868	1.938372	99.70232
123	4.49E+13	0.00E+00	0.00E+00	286	1.24E+14	0.00E+00	0.00E+00
124	4.8E+13	0.00E+00	0.00E+00	287	5.70E+15	0.00E+00	8171.387
125	6.18E+13	0.00E+00	0.00E+00	288	7.27E+09	0.475126	-949.641
126	1.1E+14	0.00E+00	1520.036	289	2.1E+12	0.43396	-190.965
127	6.53E+12	0.00E+00	-395.093	290	6.35E+12	0.00E+00	807.6686
128	4.25E+13	0.00E+00	0.00E+00	291	2.23E+12	0.00E+00	670.4175
129	2.6E+13	0.00E+00	0.00E+00	292	2.28E+14	0.00E+00	5366.155
130	5.29E+13	0.00E+00	0.00E+00	293	7.15E+10	0.252442	-512.353
131	4.54E+13	0.00E+00	0.00E+00	294	3.13E+11	0.292563	5.987804

132	1.79E+14	0.00E+00	7567.928	295	1452603	1.712963	-169.154
133	1.02E+14	0.00E+00	-288.669	296	2.58E+12	0.00E+00	840.1206
134	5.34E+13	0.00E+00	0.00E+00	297	3.33E+12	0.00E+00	890.1707
135	4.81E+12	0.00E+00	771.2729	298	3.07E+13	0.00E+00	18643.86
136	504400.1	2.074394	3691.076	299	2.16E+09	1.333883	1292.637
137	1.67E+15	0.00E+00	6258.628	300	2.03E+09	1.29416	1077.553
138	4.5E+13	0.00E+00	0.00E+00	301	2.15E+10	0.657898	-520.308
139	2790328	2.055039	4621.823	302	2.77E+12	0.00E+00	6517.533
140	8.68E+11	0.481389	2464.526	303	2548965	1.979525	3184.715
141	3.27E+13	0.00E+00	0.00E+00	304	5.07E+11	0.444103	-777.065
142	1.52E+13	0.00E+00	267.5177	305	1.43E+14	0.00E+00	0.00E+00
143	9.09E+12	0.00E+00	331.5624	306	1.81E+10	0.00E+00	0.00E+00
144	2.76E+13	0.00E+00	0.00E+00	307	2.16E+10	0.00E+00	0.00E+00
145	1.25E+13	0.00E+00	0.00E+00	308	1.88E+13	0.00E+00	0.00E+00
146	7.47E+13	0.00E+00	0.00E+00	309	1.12E+13	0.00E+00	0.00E+00
147	4.60E+17	-0.99482	601.681	310	1.19E+13	0.00E+00	0.00E+00
148	2.61E+13	0.00E+00	0.00E+00	311	3.27E+13	0.00E+00	0.00E+00
149	1.38E+13	0.00E+00	-280.057	312	1.07E+13	0.00E+00	0.00E+00
150	1.57E+13	0.00E+00	-320.655	313	216877.7	2.64574	1778.136
151	8.58E+12	0.00E+00	0.00E+00	314	1185497	2.349785	3781.631
152	7.36E+12	0.00E+00	0.00E+00	315	34666070	1.890746	435.7341
153	1.38E+13	0.00E+00	0.00E+00	316	377.0486	2.506359	697.6902
154	3.98E+13	0.00E+00	-298.822	317	0.914444	3.46501	3069.864
155	3.3E+13	0.00E+00	14040.63	318	2646300	1.552584	2935.563
156	2.28E+12	0.00E+00	8917.21	319	9.1E+13	0.00E+00	0.00E+00
157	25917.53	2.212623	2332.128	320	3.73E+13	0.00E+00	0.00E+00
158	6.68E+16	-1.35161	372.4801	321	4233056	2.237284	387.0982
159	7.43E+12	0.108114	6091.322	322	2.37E+13	0.00E+00	0.00E+00
160	2.82E+13	0.00E+00	0.00E+00	323	2.48E+10	0.239783	-406.876
161	3676.684	2.824019	3378.264	324	2.57E+13	0.00E+00	0.00E+00
162	25910443	1.63089	5186.798	325	2E+13	-0.33612	0.00E+00
163	11180608	1.389267	4699.124				

11. REFERENCES

1. Noda, T. and Foster, D.E., "A Numerical Study to Control Combustion Duration of Hydrogen-Fueled HCCI by Using Multi-Zone Chemical Kinetics Simulation", ***SAE Paper***, No. 01-0250, (2001).
2. Fiveland, S.B. and Assanis, D.N., "A Four-Stroke Homogeneous Charge Compression Ignition Engine Simulation for Combustion and Performance Studies", ***SAE Paper***, No. 01-0332, (2000).
3. Suzuki, H., Koike, N., Ishii, H. and Odaka, M., "Exhaust Purification of Diesel Engines by Homogeneous Charge with Compression Ignition Part 1: Experimental Investigation of Combustion Behavior under Premixed Homogeneous Ignition Method", ***SAE Paper***, No. 970313, (1997).
4. Ishibashi, Y. and Asai, M., "Improving the Exhaust Emission of Two- Stroke Engines by Applying the Activated Radical Combustion", ***SAE Paper***, No. 960742, (1996).

5. Ryan, T.W. and Callahan, T.J., "Homogeneous Charge Compression Ignition of Diesel Fuel", ***SAE Paper***, No. 961160, (1996).
6. Aceves, S.M., Flowers, D.L., Westbrook, C.K., Smith, J.R., Pitz, W., Dibble, R., Christensen, M. and Johansson, B., "A Multi-Zone Model for Prediction of HCCI Combustion and Emissions", ***SAE Paper***, No. 01-0327, (2000).
7. Fiveland, S.B. and Assanis, D.N., "A Four-Stroke Homogeneous Charge Compression Ignition Engine Simulation for Combustion and Performance Studies", ***SAE Paper***, No. 01-0332, (2000).
8. Easley, W.L., Agarwal, A. and Lavoie, G.A., "Modeling of HCCI Combustion and Emissions using Detailed Chemistry", **SAE Paper** no. 2001-01-1029, (2001).
9. Ogink, R. and Golovitchev, V., "Gasoline HCCI Modeling: An Engine Cycle Simulation Code with a Multi-Zone Combustion Model", ***SAE Paper***, No. 01-1745, (2002).
10. Babajimopoulos, A., Lavoie, G.A. and Assanis, D.N., "Modeling HCCI Combustion with High Levels of Residual Gas Fraction-A Comparison of Two VVA Strategies", ***SAE Paper***, No. 01-3220, (2003).
11. Kongsereeparp, P. and Checkel, M.D., "Novel Method of Setting Initial Conditions for Multi-zone HCCI Combustion Modeling", ***SAE Paper***, No. 01-0205, (2007).
12. Komninos, N.P., Hountalas, D.T. and Kouremenos, D.A., "Development of a New Multi-Zone Model for Description of Physical Processes in HCCI Engines", ***SAE Paper***, No. 01-0562, (2004).
13. Komninos, N.P., Hountalas, D.T. and Rakopoulos, C.D., "A Parametric Investigation of Hydrogen Hcci Combustion using a Multi-Zone Model approach", ***Energy Conversion and Management***, Vol. 48, (2007), 2934–2941.
14. Chang, J., Guralp, O., Filipi, Z. and Assanis, D.N., "New Heat Transfer Correlation for an HCCI Engine Derived from Measurements of Instantaneous Surface Heat Flux", ***SAE Paper***, No. 01-2996, (2004).
15. Komninos, N.P., "Investigating the Importance of Mass Transfer on The Formation of HCCI Engine Emissions using a Multi-Zone Model", ***Applied Energy***, Vol. 86, (2009), 1335–1343.
16. Aceves, S.M., Smith, J.R., Westbrook, C. and Pitz, W., "Compression Ratio Effect on Methane HCCI Combustion", ***ASME Journal of Engineering for Gas Turbines and Power***, Vol. 121, (1999), 569-574.